Coordinated Object Locating of Dual-arm Robotic System Using Marker-based Multi-view Pose Estimation for Autonomous Workpiece Loading

Po-Yu Lin, Feng-Li Lian, Yuan-Chieh Lo, Chih-Hsuan Shih, Ming-Hau Tsai, and Ping-Lang Yen

Abstract—**Industrial robots play crucial roles on machining and manufacturing automation. Recently, more and more highly repetitive and hazardous jobs have been done by industrial robots. However, current automatic machining systems by robots are still not flexible and robust enough in the workpiece-loading process. In this paper, a dual-arm robotic object-locating system equipped with a depth camera is proposed for autonomous workpiece loading to improve the flexibility and robustness of the robotic machining systems. It can automatically locate the workpiece, and then load it by inserting the gripper fingers into the grasping position. Firstly, the 6D pose of the in-hand workpiece occluded by the robotic gripper is estimated by the proposed marker-based multi-view pose estimation method based on the point pair features (PPFs). According to the estimated pose, a dual-arm pose is generated for locating grasping position of the in-hand workpiece considering the orientational constraint, and the dual-arm motion to reach that pose is planned online by a sampling-based planning algorithm. However, due to some error factors, such as system modeling error and pose estimation error, there may be a locating error which leads to loading failure. Therefore, an object-locating control strategy is developed for compensating the locating error. Illustrative experiments are conducted to evaluate the performance of the proposed methods and to verify the feasibility of the proposed system. Detailed analysis related to the experimental results is provided.**

Index Terms*—*Dual-arm robotic system, manufacturing automation, motion planning, next-best view planning, object-locating control, point pair feature, workpiece loading

I. Introduction

In recent decades, robotics has been widely used to automate manufacturing processes not only in the industrial field but also in some applications related to the daily life. It can replace human operators for highly repetitive and/or hazardous works. Moreover, stable robots or machines have the ability to work day and night without taking a break compared to human beings, which greatly increases productivity. In the industrial field, works adopt robotics for automation including welding and warehouse management to name a few. When it comes to welding, glare and harsh working environment come to mind immediately. Working in such environment for a long time may cause permanent damage to one's eyes. Therefore, robotic arms have been used to replace operators. They can automatically weld certain standardized workpieces by following the predefined trajectories. Then regarding warehouse management, in conventional method, labors play an important role in this work. They are responsible for classifying incoming cargoes, arranging them, preparing items for shipment etc. In general, these cargoes are large and heavy for human. Labors are only able to deal with few of them at a time. Consequently, most of the present warehouse systems use conveyor systems with barcode scanner for delivery and classification, and replace human operators with robotic arms for manipulating these heavy cargoes. However, there are still many issues in robotics related to manufacturing automation. In the workpiece-loading process of most of the existing systems, it is essential to design a fixture for a specific kind of workpiece so that pose of the workpieces can be located, then calibrations between surrounding equipment and planning of trajectory of the robot arm for loading these workpieces should be accomplished in advance.

In this paper, inspired by the application of robotic arm for loading workpieces for CNC machines, the idea that introducing a robot arm and a visual sensor into the robotic machining systems for automating the workpiece-loading procedure comes up. To apply the robot arm for loading workpieces for robotic machining systems, a method that solves the transfer of workpieces between robots is necessary. Thus, for simplicity, a dual-arm robotic system composed of two single-arm manipulators with visual sensory feedback is proposed and is used in this paper. It is supposed that one of the robot arms is able to conduct random bin picking. Therefore, the workpiece is initially held by that robot. In the dual-arm robotic system, two robot arms can operate not only in a non-coordinated manner, where the arms perform two independent tasks, but also in a coordinated manner, where the arms perform different parts of the same task with temporary and spatial coordination of arm movements [1]. One arm can pick up and hold the workpiece independently, and then transfer it to the other arm for machining by using the sensory information to plan and control. The main contributions provided in this work lie in the improvements of robustness and flexibility of the loading process in the original robotic machining system. In addition, some time-consuming preparatory works and costs for additional mechanisms will be saved when loading workpieces for robotic machining. In terms of the robustness of system, the proposed system can make use of the acquired visual

This research is supported by the Ministry of Science and Technology, Taiwan, under Grants: MOST 109-2221-E-002-168, MOST 109-2634-F-002-039, MOST 110-2221-E-002 -168, and by Industrial Technology Research Institute, Hsinchu, Taiwan.

Po-Yu Lin and Feng-Li Lian are with the Department of Electrical Engineering, National Taiwan University, Taipei, 10617, Taiwan, and also with the Institute of Mechanical and Mechatronics Systems, Industrial Technology Research Institute, Hsinchu, 31040, Taiwan(email: fengli@ntu.edu.tw)

Yuan-Chieh Lo, Chih-Hsuan Shih, and Ming-Hau Tsai are with Institute of Mechanical and Mechatronics Systems, Industrial Technology Research Institute, Hsinchu, 31040, Taiwan.

Ping-Lang Yen is with the Department of Biomechatronics Engineering, National Taiwan University, Taipei, 10617, Taiwan.

information to sense the surrounding changes and to estimate the pose of incoming workpiece which is grasped by one of the robot arms. Consequently, the limitation on the predetermined situations is eased. Considering the flexibility of system, the proposed system can plan and execute a feasible single-/dual-arm motion online based on the estimated in-hand object pose. The motion of robot arms is no longer constrained by the trajectories which are predefined manually by human workers.

The rest of the paper is organized as follows. Literature survey is discussed in Section II. Section III formulates the problem studied in this paper. Sections IV presents the proposed methods and approaches. Section V describes the experimental results and analysis to evaluate the method for autonomous workpiece loading. Section VI concludes this paper.

II. Literature Survey

In consequence of the advantages of low cost, high flexibility, and multi-functionality, industrial manipulators have been adopted for industrial automation and robotic machining over the past few decades [2]. With increasing research interest in these applications, there are more and more related research works regarding the robotic manufacturing. Moreover, due to recent advances in both anthropomorphic robots and bimanual industrial manipulators [1], the use of dual-/multi-arm robotic system for manufacturing has attracted a large deal of interest. In this section, research works related to dual-/multi-arm robot for manufacturing are reviewed and are classified into four categories including peg in hole [3]-[8], pick and place [9]-[14], additive manufacturing [15]-[18], and subtractive manufacturing [19]-[23].

For dual-/multi-arm peg-in-hole assembly, motion planning and control strategy are two core issues. In[3] and [4], both motion planning strategies for generating grasps and motions of a dual-arm robot and control strategies for compensating the misalignment errors between peg and hole are presented. They both use visual sensor to locate the objects and then plan grasps and motions based on objects' CAD model. Compliant control is used in [3], but PID control in [4]. In [5] and [7], motion planning problem is focused. Pose constraints of objects and robot and gravitational constraints are taken into account when planning in [5]. Manipulability Metric is optimized in [7]. In [6] and [8], control strategy for revising the reference trajectory to complete the peg-in-hole task is concentrated on. Hybrid force/position control scheme is adopted in [6], while a sparse kinematic control strategy that minimizes the number of joints actuated for a coordinated task between two arms is proposed in [8].

In pick-and-place task, some originally unachievable task requirements by a single robot arm due to limitation of robot workspace can be done now through object exchange between two or multiple robots. Thus, motion planning for regrapsing and object exchange is one of the core issues and is discussed in [9], [11], [12], and [14]. Furthermore, when both the start goal configurations of the objects can be reached by all robots in the system, scheduling and dispatching is also an important issue. In [10], part-dispatching rules are proposed to improve the productivity. In [13], a scheduling component which coordinates manipulation actions between two robot arms to minimize execution time is presented.

For additive and subtractive manufacturing, owing to additional and redundant degrees of freedom, the system can process more complex surface shape of workpiece by dual-/multi-arm cooperation. To operate in a coordinated manner, motion planning and control strategy for coordination are two main issues. In [15], an object-oriented hierarchical planning control strategy as well as a new symmetrical internal and external adaptive variable impedance control are proposed. In [16], [18], [19], and [20], there are various motion planning approaches proposed for dual-/multi-arm robotic system, such as an approach based on the closed kinematic chain model[16], an approach considering resource allocation [18], a path-constrained approach for synchronous motion by appropriately parameterizing the configuration variables [19], and an optimization method that minimizes the system compliance factor to reduce machining torques and deflection of tool [20]. In addition to motion planning and control issues, there are also a few works discussing calibration between robots' base coordinate frame and scheduling of the robotic system. In [17], a three-point calibration method of two robots' relative base coordinate system as well as a motion planning method based on non-master/slave scheme is presented. In [21], a non-contact calibration method depending on binocular vision is proposed for Multi-robot coordination grinding system. For scheduling issue, an efficient method balancing the workload of the robots and ensuring collision-free scheduling is presented in [22], and a method for energy consumption optimization by embedding evaluations of robots' energy consumptions into a scheduling model is presented in [23].

In summary, adoption of dual-/multi-arm robotic system for manufacturing can expand workspace of the whole system, improve flexibility, speed up process, etc. To achieve these benefits, there are corresponding issues should be tackled. It can be concluded that most works address motion planning problem for dual-/multi-arm robotic system. Control issue is discussed when the system is required to operate in a coordinated manner or the arms are physically interacting with one another. Calibration problem is mostly considered when the arms are not connected with each other by any mechanism, i.e., the relationship between base coordinate frames cannot be derived from CAD model. Then scheduling issue is faced when source conflicts exist. In this paper, a dual-arm robotic system for manipulating and loading workpieces in a coordinated manner is proposed. There are no additional mechanisms used to connect them. Therefore, motion planning and control issue, as well as calibration problem should all be considered, which increases the difficulty. The way that the workpiece is loaded is by inserting the gripper fingers into grasping position of the workpiece, which is similar to the peg-in-hole assembly. Similar works include [3], [4], and [6]. Compared to [3], both consider motion planning problem, but the proposed system does not require expensive F/T sensors to implement the control strategy. Compared to [4], both use vision-based control, but the proposed system considers not only positional but also orientational locating error. Compared to [6], the proposed system does not rely on collaborative robots.

III. Problem Formulation

The robots involved in the workpiece-loading process have different functions including picking, sensing, and machining. The robot with picking function picks the workpiece and tranfer

it to the robot with maching function. During the process, the robot with sensing function provides useful information. However, considering space and cost, one of the robot has both sensing and machining function in the proposed system. The proposed dual-arm robotic system is composed of two industrial manipulators which have an overlapping workspace. Each industrial manipulator has its independent robot controller in Windows operating system. Available measurements include joint states of the dual-arm robot from encoders of joint motors, and rich visual information, such as RGB images, depth images, and point cloud data, provided by a RealSense D415 RGB-D camera mounted on one of the robot arms in eye-in-hand configuration. The reason why the eye-in-hand configuration is adopted is because it can make use of degrees of freedom of the robot to sense the environment and is more flexible.

To implement the workpiece-loading task on the proposed dual-arm robotic system, challenges include pose estimation of the target workpiece which is grasped and is partially occluded by robotic gripper, online planning of collision-free and feasible dual-arm motion for locating grasping position and satisfying orientational constraint, and control strategy design to compensate the object-locating error in order for loading the workpiece successfully. An illustration of the formulated problem tackled is shown in Figure 1.

A. In-hand Object Pose Estimation

To locate grasping position of the target workpiece, current pose of the target workpiece must be estimated. In the case faced in this paper, the object has already been held by one of the robot arms, which belongs to the post-grasp case. In the pose-grasp case, in-hand object is often significantly occluded by robotic gripper, which decreases the number of visual data belongs to the target object acquired from a single view. Moreover, it is hard to distinguish the target object from the gripper by the received visual information when they look similar. Hence, in-hand object pose estimation remains challenging. In this paper, a marker-based multi-view object pose estimation algorithm is implemented to tackle this challenging problem.

B. Dual-arm Motion Planning

Considering motion planning for robotic manipulation, a desirable property is the ability to identify usable solutions quickly. In dual-/multi-arm system, the number of degrees of freedom is increased. Although more complex and dexterous manipulation tasks can be performed, the configuration space of these platforms is high-dimensional, which will increase the computational loads. In addition to the requirement to plan over such high-dimensional configuration spaces, the motion planner also has to perform computationally expensive collision checking procedures, and to take task objectives into account. Thus, quickly providing feasible plans for the manipulation problem in dual-arm system is challenging.

C. Object-locating Control Strategy Design

The dual-arm robotic system consists of two independent industrial manipulators which have their own platforms and are not connected by any mechanisms. The transformation between base frames of the robots has to be obtained by conducting calibration manually, which is inevitable that there will be calibration errors. In consequence, the object is usually not located well because planning of the robot poses used for locating object involves this transformation, not to mention that the robotic system also contains other potential error factors such as estimation error of the object pose. Thus, an object-locating control strategy should be developed and used to decrease the error so that the workpiece can be loaded successfully.

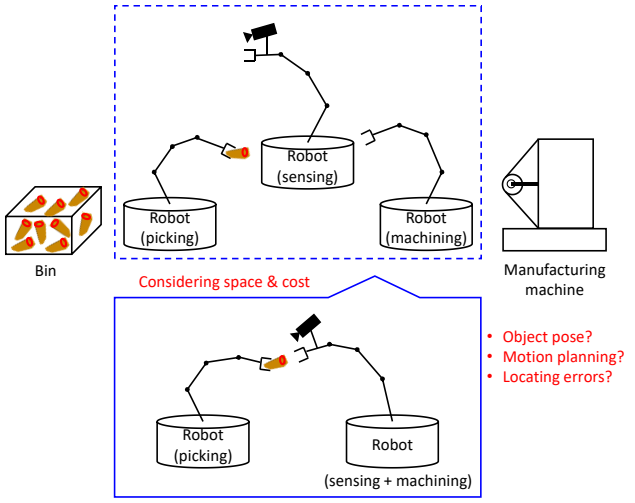

Figure 1. Schematic diagram of the formulated problem.

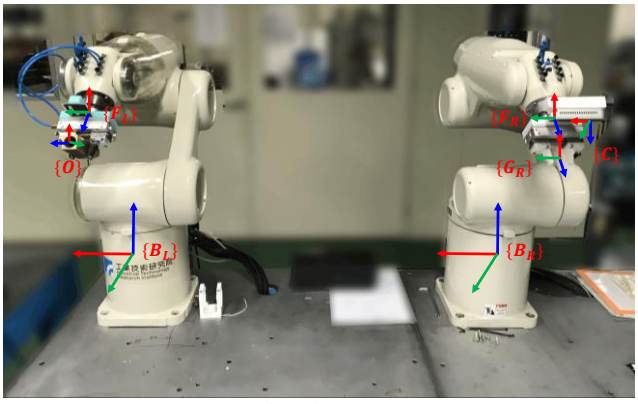

Figure 2. Schematic diagram of the formulated problem.

In Figure 2, the primary coordinate systems are shown with their notations. Frame $\{B_L\}$ and $\{B_R\}$ are the base frames of the left arm and the right arm, respectively. Here, the base frame of the left arm is looked upon as the world frame of the whole system. All data represented in the local reference frames are usually transformed into the world frame before other processes such as motion planning. Frame $\{F_L\}$ and $\{F_R\}$ represent the flange frames of the left arm and right arm, respectively. Frame $\{C\}$ denotes the camera coordinate system. In addition, frame $\{G_R\}$ is the gripper frame of the right arm, which is extended from frame $\{F_R\}$. The relation between frame $\{G_R\}$ and $\{F_R\}$ is determined directly by 3D CAD models of the gripper and the adapter. Finally, frame {O} is the workpiece frame. The pose estimation result is exactly the transformation between the workpiece frame and the world frame.

IV. Object Pose Estimation and Object Locating

In Figure 3, an overview of the proposed method is shown. There are two main portions: pose estimation for in-hand workpiece (blue block) and dual-arm object locating (red block). Pose of the in-hand workpiece is estimated by the proposed marker-based multi-view pose estimation method. After that, the estimated pose of the in-hand workpiece ${}^{B_L}_{O}\boldsymbol{T}$ will then be

the input of the dual-arm object locating to locate the workpiece. These two portions are introduced in the following two subsections, respectively.

A. Marker-based Multi-view Pose Estimation

The dual-arm robot firstly moves to a predefined initial pose to make the camera which is installed on one of the robot arms perceive the marker which is attached to the other one near the target object. The marker called ArUco marker is a synthetic square marker composed by a wide black border and an inner binary matrix which determines its identifier. In this way, position of the marker $\boldsymbol{p_{POI}}$ can be estimated and will be used for the following next-best view planning and point cloud segmentation. After that, the method enters the active vision loop composed of scene updating, next-best view planning, and motion planning to acquire visual data from multiple views. In the active vision loop, only the robot with visual sensor will move. In the scene updating stage, the perceived point cloud from the current view is briefly segmented according to the position of the marker by

$$\begin{cases} x_{min} \le x_i \le x_{max} \\ y_{min} \le y_i \le y_{max}, \\ z_{min} \le z_i \le z_{max} \end{cases} \tag{1}$$

where x_{min}, x_{max}, y_{min}, y_{max}, z_{min}, and z_{max} are user-defined parameters according to the prior knowledge of the hardware setup and $\boldsymbol{p_{POI}}$, and these parameters define a 3-dimensional bounding box. Points with coordinates that satisfies (1) will be kept otherwise filtered out. After that, it is sent to the octomap server to update the occupancy map [24] and surface normals of points received from the current view are estimated before being fused together with point clouds from other views. In the next-best view planning stage, the position of the marker and the occupancy map are taken as inputs to plan the next-best viewpoint. The proposed marker-based next-best view planning strategy contains three steps, sampling of candidate views, making evaluations, and selecting the next-best view.

1) Generation of Candidate Views

In order to parameterize the generation of candidate views such that the generation can be easily tunable as well as to particularly make the sensor concentrate on a certain area, a spherical coordinate system is introduced as shown in Figure 4. Position of the marker $\boldsymbol{p_{POI}}$ obtained by estimating pose of the marker is taken as the input, is viewed as the point of interest, and is served as the origin of sphere. Position of each candidate view $\boldsymbol{p_{rayo}}$ can then be parameterized as

$$\boldsymbol{p_{rayo}} = \begin{bmatrix} r\sin\theta\cos\varphi \\ r\sin\theta\sin\varphi \\ r\cos\theta \end{bmatrix}, \tag{2}$$

where r is the Euclidean distance from $\boldsymbol{p_{POI}}$ to $\boldsymbol{p_{rayo}}$, θ is the polar angle between the zenith direction and the line segment $\overline{\boldsymbol{p_{POI}}\boldsymbol{p_{rayo}}}$, and φ is the azimuthal angle measured from the azimuth reference direction to the orthogonal projection of the line segment $\overline{\boldsymbol{p_{POI}}\boldsymbol{p_{rayo}}}$ on the reference plane. For sampling orientation of each candidate view, the unit vector in the direction of increasing polar angle $\boldsymbol{e_\theta}$ is used, which is defined as

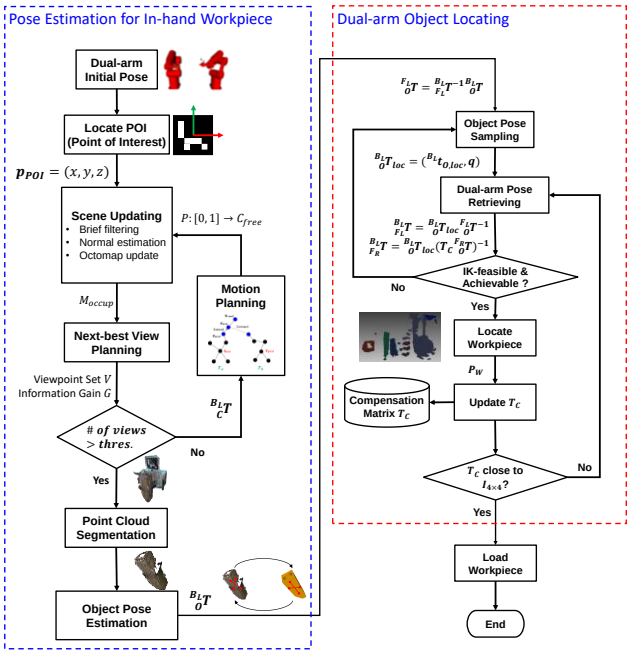

Figure 3. An overview of the proposed method.

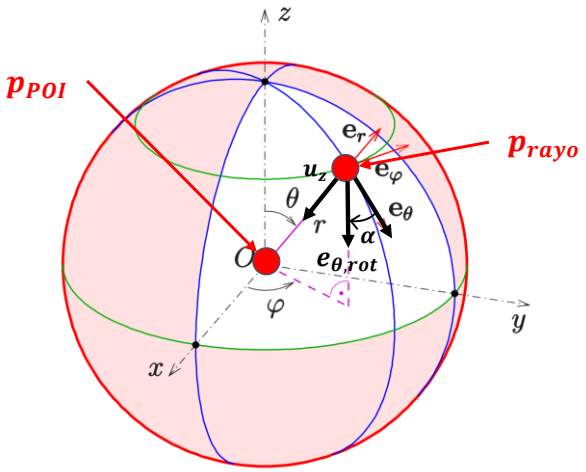

Figure 4. An illustration of the spherical coordinate system used to parameterize candidate views.

$$\boldsymbol{e_\theta} = \begin{bmatrix} \cos\theta\cos\varphi \\ \cos\theta\sin\varphi \\ -\sin\theta \end{bmatrix}. \tag{3}$$

The unit vector in z direction of the candidate views is given by

$$\boldsymbol{u_z} = \frac{\boldsymbol{p_{POI}} - \boldsymbol{p_{rayo}}}{\|\boldsymbol{p_{POI}} - \boldsymbol{p_{rayo}}\|}. \tag{4}$$

Then $\boldsymbol{e_\theta}$ is rotated around $\boldsymbol{u_z}$ by an rotation angle α for different orientations at the same position:

$$\begin{aligned} \boldsymbol{e_{\theta,rot}} &= AngleAxis(\alpha, \boldsymbol{u_z})\boldsymbol{e_\theta} \\ &= (\cos\alpha)\boldsymbol{e_\theta} + (\sin\alpha)(\boldsymbol{u_z} \times \boldsymbol{e_\theta}) + (1 \\ &\quad - \cos\alpha)(\boldsymbol{u_z} \times \boldsymbol{e_\theta})\boldsymbol{u_z}. \end{aligned} \tag{5}$$

After that, the unit vectors in x and y direction of the candidate views are computed as

$$\boldsymbol{u_x} = \frac{\boldsymbol{e_{\theta,rot}} - (\boldsymbol{e_{\theta,rot}} \cdot \boldsymbol{u_z})\boldsymbol{u_z}}{\left\|\boldsymbol{e_{\theta,rot}} - (\boldsymbol{e_{\theta,rot}} \cdot \boldsymbol{u_z})\boldsymbol{u_z}\right\|} \tag{6}$$

$$\boldsymbol{u_y} = \frac{\boldsymbol{u_z} \times \boldsymbol{u_x}}{\|\boldsymbol{u_z} \times \boldsymbol{u_x}\|}. \tag{7}$$

Therefore, the candidate views can be represented as

$$\boldsymbol{v} = \begin{bmatrix} \boldsymbol{u_x} & \boldsymbol{u_y} & \boldsymbol{u_z} & \boldsymbol{p_{rayo}} \\ 0 & 0 & 0 & 1 \end{bmatrix} \tag{8}$$

The tunable parameters include radius r, polar angle θ, azimuthal angle φ, and rotation angle α. By approiately setting these parameters, the generation of candidate views can be done.

2) Simulation of Visual Perception

After generation of the candidate views, next step is to perform simulation of visual perception on each candidate view and to estimate the amount of information can be received from each candidate view. In this strategy, a ray-tracing simulation is conducted with the occupancy map as input which is represented by Octomap [24]. Ray-tracing simulation casts multiple rays in field of view of the camera in a discretized way from the origin of each candidate view (see Figure 5). These rays may intersect the occupancy map with some voxels. Centers of the intersected voxels as well as their logits of occupancy probability are extracted as points and represent the amount of information perceived from the candidate view. The intersected points are either unknown or occupied according to their logits of occupancy probability I. For each point $\boldsymbol{p_i}$, if its absolute value of I_i is within a threshold ε_{occu}, it is unknown; Otherwise, it is occupied.

$$\text{Type of point } \boldsymbol{p_i} = \begin{cases} \text{Unknown}, & \text{if } |I_i| < \varepsilon_{occu} \\ \text{Occupied}, & \text{otherwise} \end{cases} \tag{9}$$

3) Selection of Next-best View

To choose the next-best viewpoint from the candidate views, an evaluation metric is necessary to judge them. Here, the metric used is designed by the concept of information gain. First, each type of point is assigned a weight. Then, the candidate views are evaluated by summation of weights of all the perceived points. More specifically, for a candidate view $\boldsymbol{v_i}$, its metric value G_i is defined as

$$G_i = \sum_{\boldsymbol{p_i} \text{ visible from } \boldsymbol{v_i}} \begin{cases} 1, & \text{if } \boldsymbol{p_i} \text{ is unknown} \\ -0.2, & \text{otherwise} \end{cases} \tag{10}$$

The one reachable and with larger metric value G is chosen as the next-best viewpoint. If the termination condition is not satisfied, motion planning is executed to find a trajectory for the robot arm which has the camera reach the feasible next-best view to scan the scene. The termination condition in this work is the number of next-best views used to acquire information. If the number of next-best views used exceeds a threshold, the active vision loop ends.

After ending the active vision loop for acquiring visual information from multiple views, the interested point cloud which may belong to the target object and is used for 6D object pose estimation is segmented with the help of the pose of the marker by (1). In this paper, the point pair feature (PPF) proposed by [25] is used to register 3D CAD model of the object to the object point cloud for obtaining object pose. For the sake of efficiency, the method extracts PPFs of the object model and

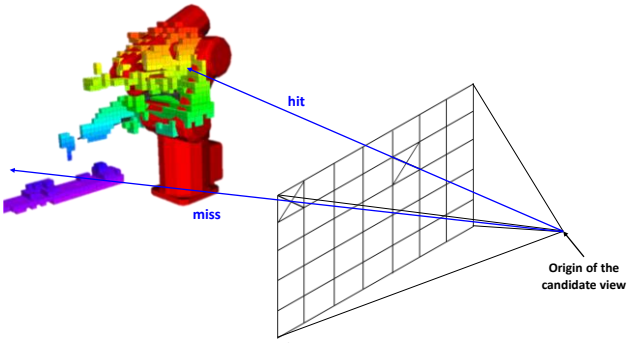

Figure 5. A schematic diagram of ray-tracing simulation.

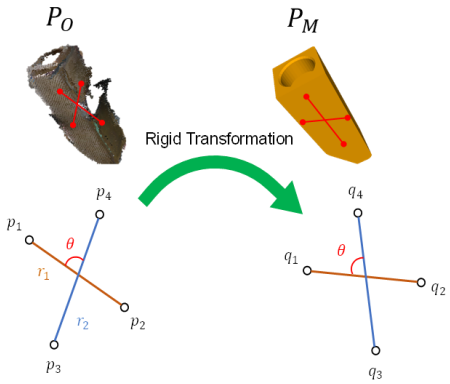

Figure 6. Matching bases between the object's point cloud segment and the model's point cloud.

constructs a hash map offline for online estimating process. In the online matching process, sets of 4-point co-planar bases are sampled on the object's point cloud segment (P_O), and the congruent sets are searched on the model's point cloud (P_M) to generate object pose hypotheses with the help of the hash map (Figure 6). After getting the pose hypotheses, post-processing techniques including pose clustering and iterative closest point are applied on the hypothesis set to generate the final estimation result ${}^{B_L}_{O}\boldsymbol{T}$.

B. Dual-arm Object Locating

After finishing the proposed marker-based multi-view pose estimation, pose of the in-hand workpiece ${}^{B_L}_{O}\boldsymbol{T}$ is estimated and is then taken as the input to generate a dual-arm pose for locating grasping position of the workpiece. The dual-arm pose is generated through retrieving from the corresponding pose of the workpiece which is gripped. In other words, a workpiece pose ${}^{B_L}_{O}\boldsymbol{T}_{loc}$ will be sampled first in the shared workspace. After that, by considering the estimated relationship ${}^{F_L}_{O}\boldsymbol{T}$ and the loading constraint ${}^{F_R}_{O}\boldsymbol{T}$ between the workpiece and the flanges, a set of robot poses $({}^{B_L}_{F_L}\boldsymbol{T}, {}^{B_L}_{F_R}\boldsymbol{T})$ is retrieved as follows:

$$\begin{aligned} {}^{B_L}_{F_L}\boldsymbol{T} &= {}^{B_L}_{O}\boldsymbol{T}_{loc}\, {}^{F_L}_{O}\boldsymbol{T}^{-1} \\ {}^{B_L}\boldsymbol{T} &= {}^{B_L}_{O}\boldsymbol{T}_{loc}(\boldsymbol{T_C}\, {}^{F_R}_{O}\boldsymbol{T})^{-1}, \end{aligned} \tag{11}$$

where $\boldsymbol{T_C}$ is the compensation matrix which is initially an identity matrix and is introduced later. If both robot poses are IK-feasible and achievable checked by RRT-Connect algorithm [26], both robots will move to the retrieved dual-arm pose to

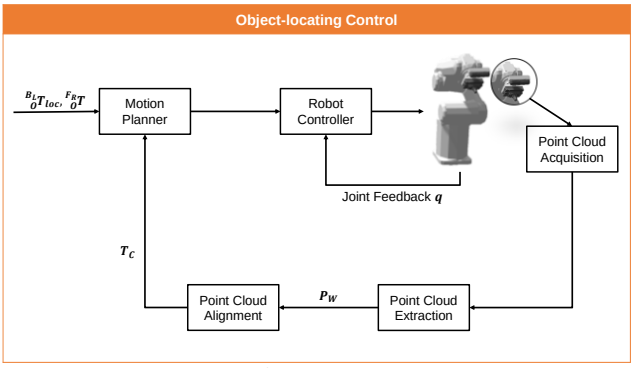

Figure 7. The block diagram of the object-locating control strategy.

initially locate the object and the procedure moves on to the object-locating control loop. Otherwise, it will turn back to sample a new workpiece pose and retrieve a new set of robot poses.

The concept of this object-locating control strategy is to maintain a matrix $\boldsymbol{T_C}$ which estimates the current deviation from the ideal pose, and then use it to adjust the pose of the robot with visual sensor for compensation by using (11) to retrieve it again. Block diagram of object-locating control strategy is shown in Figure 7. At the beginning, $\boldsymbol{T_C}$ is initialized to an identity matrix. In each round, after the robot with visual sensor moves to the retrieved pose, $\boldsymbol{T_C}$ is updated by making use of the point cloud data generated from the depth camera. First, points belong to the workpiece among the captured point cloud are segmented by a color-based algorithm, and are transformed into the frame $\{F_R\}$. With the points of the workpiece $\boldsymbol{P_W}$, $\boldsymbol{T_C}$ can then be obtained by using the ICP algorithm [27], a local registration algorithm, to align these points to the workpiece model which is transformed by the loading constraint ${}^{F_R}_{O}\boldsymbol{T}$. The robots will continually adjust their end-effector's poses by using and updating $\boldsymbol{T_C}$ until $\boldsymbol{T_C}$ is close enough to the identity matrix as shown in Figure 3, which means the adjustment is small enough and the constraint ${}^{F_R}_{O}\boldsymbol{T}$ is considered to be satisfied. The conditions used to determine the similarity between $\boldsymbol{T_C}$ and the identity matrix are designed as follows:

$$\begin{cases} |\alpha| < 1.0° \\ |\beta| < 1.0° \\ |\gamma| < 1.0° \\ \delta = \sum_{\boldsymbol{p_i} \in \boldsymbol{P_W}} \frac{1}{N} \|\boldsymbol{p_i} - \boldsymbol{T_C p_i}\| < 5 \times 10^{-3} \end{cases} \tag{12}$$

where α, β, and γ are Euler angles of the rotational part of $\boldsymbol{T_C}$, δ is the average translational difference before and after $\boldsymbol{P_W}$ being transformed by $\boldsymbol{T_C}$, and N is the total number of points in $\boldsymbol{P_W}$. Once these conditions are satisfied, the final application is executed.

V. Experiments

In Figure 8, experimental setup of the dual-arm robotic platform used for validation is shown. The platform is composed of two ITRI AR605 industrial robots, an Intel RealSense D415 depth camera, an ArUco marker, and HCG faucet part. Each ITRI AR605 industrial robot has six degrees-

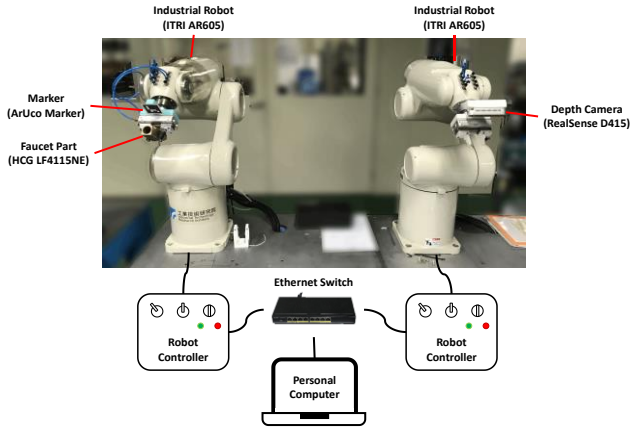

Figure 8. Experimental setup of the dual-arm robotic platform.

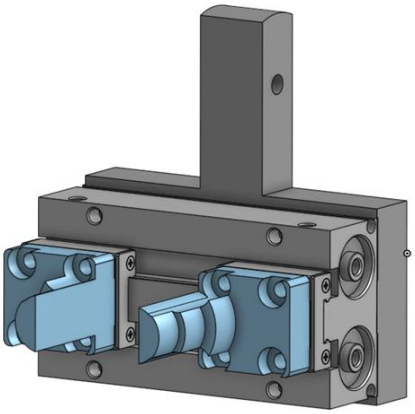

Figure 9. A closed-up view of the grasping mechanism.

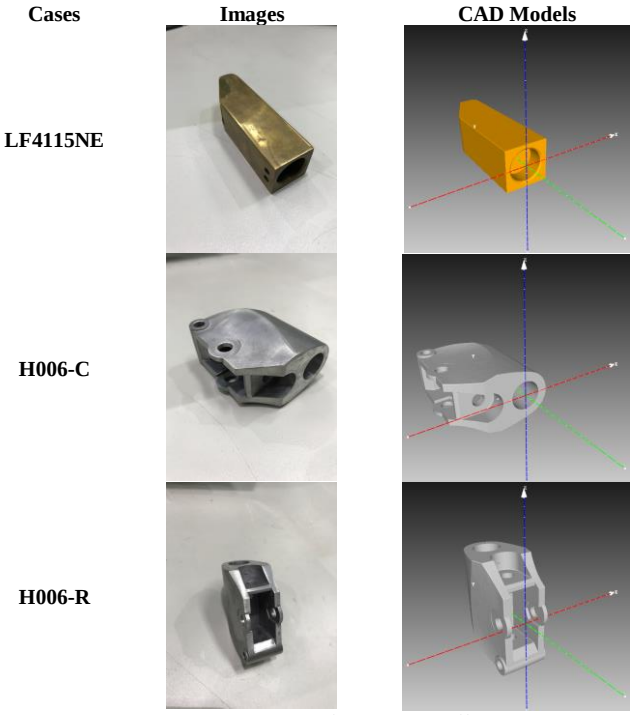

Figure 10. Images and CAD models of these three different cases adopted in the workpiece-loading application.

Table I: Experimental cases in robotic workpiece loading.

Case	Object-locating Control	Shape of Workpiece (H × W × D)	Shape of Grasping Position	Exp. times
LF4115NE	Without	0.0280m × 0.0284m × 0.096m	Circular	10
	With			
H006-C	Without	0.0372m × 0.0611m × 0.0711m	Circular	10
	With			
H006-R	Without	0.0372m × 0.0611m × 0.0711m	Rectangular	10
	With			

of-freedom, 6 kg maximum payloads, and a robot controller. The robot controller is position-based and cannot be controlled in torque mode. In addition, the robot consists of rigid links. Therefore, it is not compliant. The RealSense D415 depth camera is mounted on the right robot arm to acquire surrounding visual data, which forms the eye-in-hand configuration. The ArUco marker used to locate the point of interest when sampling candidate views is attached to the gripper adapter of the left robot arm which is designed to connect the flange with the parallel gripper (Figure 9). The target workpiece is the HCG faucet part (product type: LF4115NE). A personal computer is served as the upper-level controller which is responsible for all planning and computations and connects to both robot controllers through an Ethernet switch.

To verify the applicability of the proposed system to workpiece loading, there are two more cases designed for experiments considering shapes of the workpiece and of the grasping position in addition to the HCG faucet part. Images and CAD models with coordinate systems visualized of these three cases are shown in Figure 10. It can be seen that y-axis in all coordinate systems points towards the grasping positions. This is designed purposely. In this way, the loading constraint ${}^{F_R}_{O}\boldsymbol{T}$ used to retrieve the robot poses is the same in all the cases and is defined as

$$ {}^{F_R}_{O}\boldsymbol{T} = \begin{bmatrix} 1 & 0 & 0 & 0 \\ 0 & 0 & -1 & 0 \\ 0 & 1 & 0 & 0.45 \\ 0 & 0 & 0 & 1 \end{bmatrix}. \tag{13} $$

Experiments are conducted with and without the proposed object-locating control strategy, and each case is executed ten times to compute its success rate and to valid the proposed method. A workpiece-loading trial is regarded as successful if the gripper fingers are inserted smoothly into the grasping position without serious collision with the workpiece. Table I lists and summarizes these cases. The experimental procedure is illustrated in Figure 11.

A. Without Object-locating Control

In this section, the trials conducted without the proposed object-locating strategy are demonstrated. The experimental results obtained from the first trial in each case are shown in Table II. Firstly, the pose estimation result ${}^{B_L}_{O}\boldsymbol{T}$ is presented by using the CAD model and the final point cloud fusion result. The CAD model is transformed into the same coordinate frame with the fused point cloud's by ${}^{B_L}_{O}\boldsymbol{T}$ to demonstrate the result.

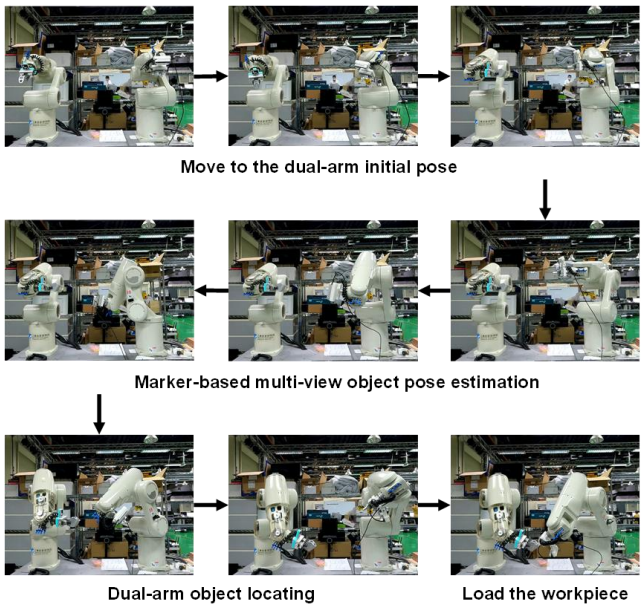

Figure 11. An illustration of the experimental procedure.

Table II: The experimental results obtained from the first trial in each case without object-locating control.

Case	${}^{B_L}_{O}\boldsymbol{T}$	$\boldsymbol{P_W}$ (initial locate)	Result
LF4115NE		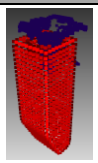	
H006-C	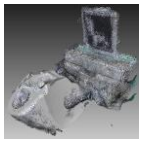	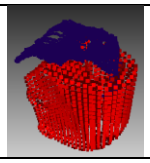	
H006-R		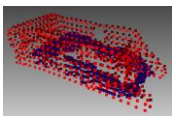	

Table III: Summary of the workpiece-loading results of these ten trials in different cases without object-locating control.

Case	T 1	T 2	T 3	T 4	T 5	T 6	T 7	T 8	T 9	T 10
LF4115NE	X	X	X	X	X	X	X	X	X	X
H006-C	X	X	X	X	X	X	X	X	X	X
H006-R	X	O	O	O	X	X	X	O	X	X

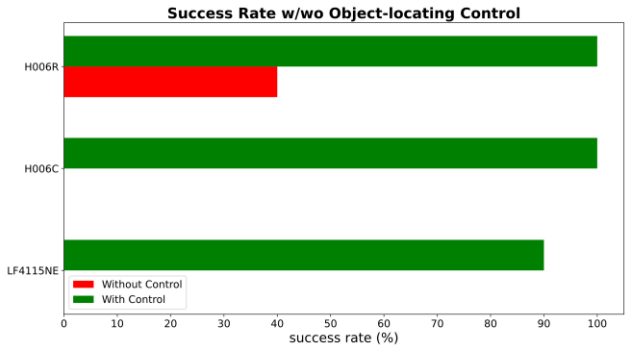

Figure 12. Success rates of the workpiece-loading application in these three cases w/wo the object-locating control strategy.

After moving to the initial locating poses, point cloud of the workpiece $\boldsymbol{P_W}$ is extracted and transformed into the frame $\{F_R\}$. The figures displayed in Table II show $\boldsymbol{P_W}$ (dark blue) together with the workpiece model (red) which is transformed into the expected pose by the loading constraint ${}^{F_R}_{O}\boldsymbol{T}$. It can be seen that $\boldsymbol{P_W}$ is not very matched with the model, which means the workpiece is not actually at the expected pose and ${}^{F_R}_{O}\boldsymbol{T}$ is not satisfied. Because the object-locating control strategy for compensating the locating errors is not applied, the procedure will move on to the loading process. The robots will directly attempt to load the workpiece. The results of the first trail in these three cases are demonstrated in the last column of Table II. They are all failed to load the workpiece. Moreover, the loading results of all trials in these three cases are organized in Table III.

B. With Object-locating Control

In this section, the trials conducted with the proposed object-locating strategy are demonstrated. The difference with the previous section lies after the robots reach the initial locating poses. In previous section, the procedure moves on to the final workpiece-loading process. However, in this section, the procedure enters a feedback loop as shown in Figure 3 to maintain the compensation matrix $\boldsymbol{T_C}$ and adjust the robot poses, which aims to fix the locating errors. The loop will not end until the termination conditions listed in (12) are satisfied. The final workpiece-loading process is then executed. In Table IV, the experimental results obtained from the first trial in each case are also shown. The pose estimation result ${}^{B_L}_{O}\boldsymbol{T}$ is firstly presented by using the CAD model and the final point cloud fusion result. After that, point clouds of the workpiece $\boldsymbol{P_W}$ extracted after reaching the initial locating poses and in the final round of the loop are both shown. It can be obviously seen that point clouds of the workpiece become more matched with the model at the expected pose after terminating the loop, which means the locating errors is compensated. The results of the first trail in these three cases are also demonstrated in the last column of Table IV. They load the workpiece successfully.

The success rates of all cases are summarized and visualized in Figure 12. Without the proposed control strategy, all trials in case LF4115NE and H006-C are failed. In case H006-R, the success rate is 40%. Nevertheless, after applying the object-locating control strategy, the success rates of case H006-C and H006-R become 100% and the success rate of case LF4115NE becomes 90%. It can be seen that the object-locating control strategy greatly improves the performance of the application.

Table IV: The experimental results obtained from the first trial in each case with object-locating control.

Case	${}^{B_L}_{O}\boldsymbol{T}$	$\boldsymbol{P_W}$ (initial locate)	$\boldsymbol{P_W}$ (final round)	Result
LF4115NE		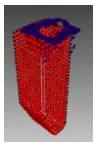	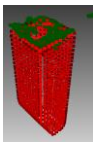	
H006-C	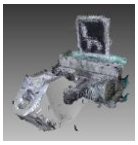	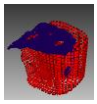	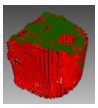	
H006-R	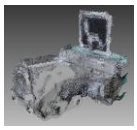			

Also, from the variations of the metrics used in the termination conditions shown in Figure 13, it can be observed that the locating errors are actually compensated.

Finally, sizes of the grasping positions of different cases and sizes of the gripper fingers in different layers are measured. Tolerances in these three cases are computed and listed in Table V. From these experimental results, it can be concluded that the proposed method is valid for estimating the in-hand object pose and fixing the locating errors such that the workpiece is well-located. The proposed dual-arm robotic system is applicable to the robotic workpiece-loading application with accuracy around ± 1 millimeters.

VI. Conclusion

In this paper, a dual-arm robotic object-locating system equipped with a RGB-D camera for autonomous workpiece loading is presented. The system can automatically locate the workpiece, and then load it by inserting the gripper fingers into the grasping position. Firstly, the marker-based multi-view pose estimation method based on point pair features (PPFs) is proposed to estimate 6D pose of the in-hand workpiece occluded by the robotic gripper. The method acquires more visual information related to the workpiece for pose estimation from multiple viewpoints planned by the next-best view planning with the help of marker. After that, based on the estimated pose, a feasible set of robot poses is generated for locating grasping position of the in-hand workpiece considering the robot kinematics and the orientational constraint. Then, a dual-arm motion to reach these robot poses is planned online by a sampling-based planning algorithm and is executed. Nonetheless, because there may be locating errors due to some

Table V: Tolerances in the workpiece-loading case.

Case	LF4115NE	H006-C	H006-R
Tolerance (mm)	± 1.09	± 1.665	$\pm 6.51 \times \pm 1.205$

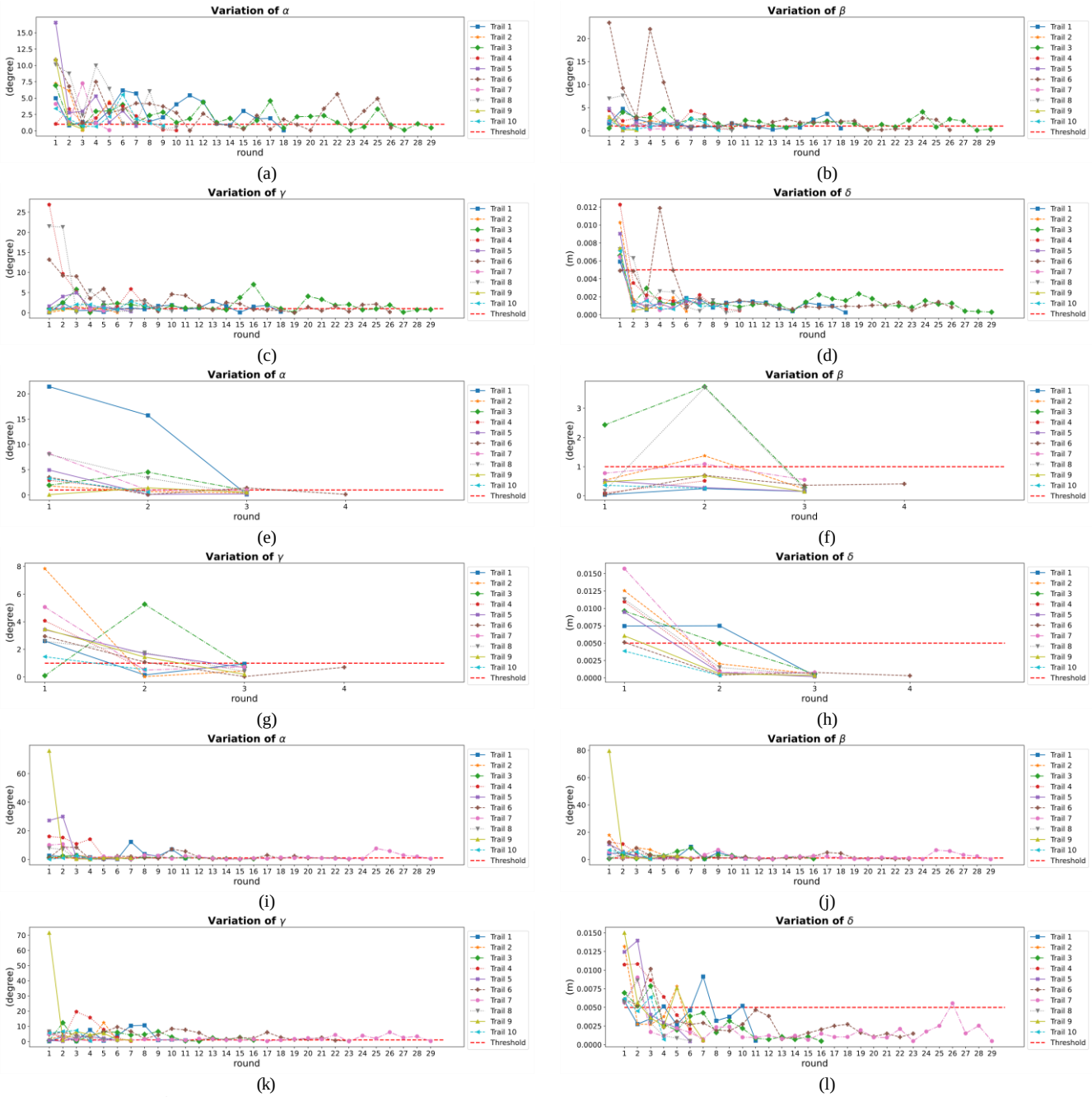

Figure 13. Variations of the metrics in the termination conditions in ten trials. (a)-(d): Case LF4115NE. (e)-(h): Case H006-C. (i)-(l): Case H006-R.

error factors, such as system modeling error and pose estimation error, an object-locating control strategy based on visual feedback is developed for compensating the locating errors in this paper. The final loading process is conducted after termination conditions of the feedback loop are satisfied.

The experimental results demonstrate the feasibility of the proposed marker-based multi-view pose estimation method and object-locating strategy. Effect of the object-locating control strategy is evaluated by conducting the workpiece-loading application on three different cases. The success rates of these three cases are greatly increased by the object-locating control strategy from almost 0% to around 100%. With the object-locating control strategy, accuracy of the robotic workpiece-loading application can achieve around ±1 millimeters. Under the premise that one of the robot arms is able to conduct random bin picking, the limitation on the predetermined situations is eased, and there is no longer any requirement to additionally design fixtures to locate the workpieces precisely and to predefine robot trajectories manually. Position and orientation of the workpiece in the shared workspace when being loaded can be flexibly adjusted according to the task objectives and constraints.

Future works include ensuring the synchronous dual-arm behavior to improve the system security, as well as leveraging machine learning techniques to improve the point cloud segmentation. In addition, because it is hard to implement other systems or methods which are related to the proposed one without required hardware and released codes of their methods,

it is difficult to make a comparison between each other on their performances using the experiments considered in this thesis. If standard validation procedures about robotic workpiece loading can be established, the comparison will be easier to do.

REFERENCES

[1] Christian Smith, Yiannis Karayiannidis, Lazaros Nalpantidis, Xavi Gratal, Peng Qi, Dimos V. Dimarogonas, and Danica Kragic, "Dual arm manipulation—A survey," Robotics and Autonomous Systems, Vol. 60, No. 10, pp. 1340-1353, Oct. 2012.

[2] Wei Ji and Lihui Wang, "Industrial robotic machining: a review," The International Journal of Advanced Manufacturing Technology, Vol. 103, No. 1-4, pp. 1239-1255, Apr. 2019.

[3] Hao Chen, Juncheng Li, Weiwei Wan, Zhifeng Huang, and Kensuke Harada, "Integrating Combined Task and Motion Planning with Compliant Control," International Journal of Intelligent Robotics and Applications, Vol. 4, No. 2, pp. 149-163, Jun. 2020.

[4] Yanjiang Huang, Xianmin Zhang, Xunman Chen, and Jun Ota, "Vision-guided peg-in-hole assembly by Baxter robot," Advances in Mechanical Engineering, Vol. 9, No. 12, 2017.

[5] Ryota Moriyama, Weiwei Wan, and Kensuke Harada, "Dual-arm Assembly Planning Considering Gravitational Constraints," in Proceedings of IEEE/RSJ International Conference on Intelligent Robots and Systems, Macau, China, pp. 5566-5572, Nov. 4-8, 2019.

[6] Matteo Parigi Polverini, Andrea Maria Zanchettin, and Paolo Rocco, "A constraint-based programming approach for robotic assembly skills implementation," Robotics and Computer-Integrated Manufacturing, Vol. 59, pp. 69-81, Oct. 2019.

[7] Sotiris Stavridis and Zoe Doulgeri, "Bimanual Assembly of Two Parts with Relative Motion Generation and Task Related Optimization," in Proceedings of IEEE/RSJ International Conference on Intelligent Robots and Systems, Madrid, Spain, pp. 7131-7136, Oct. 1-5, 2018.

[8] Sonny Tarbouriech, Benjamin Navarro, Philippe Fraisse, André Crosnier, Andrea Cherubini, and Damien Sallé, "Dual-arm relative tasks performance using sparse kinematic control," in Proceedings of IEEE/RSJ International Conference on Intelligent Robots and Systems, Madrid, Spain, pp. 6003-6009, Oct. 1-5, 2018.

[9] Yukiyasu Domae, Akio Noda, Tatsuya Nagatani, and Weiwei Wan, "Robotic General Parts Feeder: Bin-picking, Regrasping, and Kitting," in Proceedings of IEEE International Conference on Robotics and Automation, Paris, France, pp. 5004-5010, 31 May – 31 Aug., 2020.

[10] Yanjiang Huang, Ryosuke Chiba, Tamio Arai, Tsuyoshi Ueyama, and Jun Ota, "Robust multi-robot coordination in pick-and-place tasks based on part-dispatching rules," Robotics and Autonomous Systems, Vol. 64, pp. 70-83, Feb. 2015.

[11] Jean-Philippe Saut, Mokhtar Gharbi, Juan Cortés, Daniel Sidobre, and Thierry Siméon, "Planning Pick-and-Place tasks with two-hand regrasping," in Proceedings of IEEE/RSJ International Conference on Intelligent Robots and Systems, Taipei, Taiwan, pp. 4528-4533, Oct. 18-22, 2010.

[12] Rahul Shome and Kostas E. Bekris, "Anytime Multi-arm Task and Motion Planning for Pick-and-Place of Individual Objects via Handoffs," in Proceedings of International Symposium on Multi-Robot and Multi-Agent Systems, New Brunswick, NJ, USA, pp. 37-43, Aug. 22-23, 2019.

[13] Max Schwarz, Christian Lenz, Germán Martín García, Seongyong Koo, Arul Selvam Periyasamy, Michael Schreiber, and Sven Behnke, "Fast Object Learning and Dual-arm Coordination for Cluttered Stowing, Picking, and Packing," in Proceedings of IEEE International Conference on Robotics and Automation, Brisbane, Australia, pp. 3347-3354, May 21-25, 2018.

[14] Kensuke Harada, Torea Foissotte, Tokuo Tsuji, Kazuyuki Nagata, Natsuki Yamanobe, Akira Nakamura, and Yoshihiro Kawai, "Pick and Place Planning for Dual-Arm Manipulators," in Proceedings of IEEE International Conference on Robotics and Automation, Saint Paul, Minnesota, USA, pp. 2281-2286, May 14-18, 2012.

[15] Yahui Gan, Jinjun Duan, Ming Chen, and Xianzhong Dai, "Multi-Robot Trajectory Planning and Position/Force Coordination Control in Complex Welding Tasks," Applied Sciences, Vol. 9, No.5, Mar. 2019.

[16] B. Zhou, L. Xu, Z. Meng, and X. Dai, "Kinematic Cooperated Welding Trajectory Planning for Master-slave Multi-robot Systems," in Proceedings of Chinese Control Conference, Chengdu, China, pp. 6369-6374, Jul. 27-29, 2016.

[17] T. Zhang and F. Ouyang, "Offline motion planning and simulation of two-robot welding coordination," Frontiers of Mechanical Engineering, Vol. 7, No. 1, pp. 81-92, 2012.

[18] Stefania Pellegrinelli, Nicola Pedrocchi, Lorenzo Molinari Tosatti, Anath Fischer, and Tullio Tolio, "Multi-robot spot-welding cells for car-body assembly: Design and motion planning," Robotics and Computer-Integrated Manufacturing, Vol. 44, pp. 97-116, Apr. 2017.

[19] Ariyan M. Kabir, Alec Kanyuck, Rishi K. Malhan, Aniruddha V. Shembekar, Shantanu Thakar, Brual C. Shah, and Satyandra K. Gupta, "Generation of Synchronized Configuration Space Trajectories of Multi-Robot Systems," in Proceedings of IEEE International Conference on Robotics and Automation, Montreal, Canada, pp. 8683-8690, May 20-24, 2019.

[20] W.S. Owen, E.A. Croft, B. Benhabib, "A multi-arm robotic system for optimal sculpting," Robotics and Computer-Integrated Manufacturing, Vol. 24, No. 1, pp. 92-104, Feb. 2008.

[21] Chengming Ruan, Xing Gu, Youhao Li, Gong Zhang, Weijun Wang, and Zhicheng Hou, "Base Frame Calibration for Multi-robot Cooperative Grinding Station by Binocular Vision," in Proceedings of International Conference on Robotics and Automation Engineering, Shanghai, China, pp. 115-120, Dec. 29-31, 2017.

[22] Veniamin Tereshchuk, John Stewart, Nikolay Bykov, Samuel Pedigo, Santosh Devasia, and Ashis G. Banerjee, "An Efficient Scheduling Algorithm for Multi-Robot Task Allocation in Assembling Aircraft Structures," IEEE Robotics and Automation Letters, Vol. 4, No. 4, pp. 3844-3851, Oct. 2019.

[23] Alberto Vergnano, Carl Thorstensson, Bengt Lennartson, Petter Falkman, Marcello Pellicciari, Francesco Leali, and Stephan Biller, "Modeling and Optimization of Energy Consumption in Cooperative Multi-Robot Systems," IEEE Transactions on Automation Science and Engineering, Vol. 9, No. 2, pp. 423-428, Apr. 2012.

[24] Armin Hornung, Kai M. Wurm, Maren Bennewitz, Cyrill Stachniss, and Wolfram Burgard, "OctoMap: A Probabilistic, Flexible, and Compact 3D Map Representation for Robotic Systems," Autonomous Robots, Vol. 34, No. 3, pp. 189-206, Apr. 2013.

[25] Bertram Drost, Markus Ulrich, Nassir Navab, and Slobodan Ilic, "Model Globally, Match Locally: Efficient and Robust 3D Object Recognition," IEEE Computer Society Conference on Computer Vision and Pattern Recognition, San Francisco, CA, USA, pp. 998-1005, Jun. 13-18, 2010.

[26] J.J. Kuffner and S.M. LaValle, "RRT-Connect: An Efficient Approach to Single-Query Path Planning," in Proceedings of IEEE International Conference on Robotics and Automation, San Francisco, CA, USA, pp. 995-1001, Apr. 24-28, 2000.

[27] Kok-Lim Low, "Linear Least-Squares Optimization for Point-to-Plane ICP Surface Registration," Department of Computer Science, University of North Carolina at Chapel Hill, Tech. Rep. TR 04-004, Feb. 2004.

Po-Yu Lin was born in Yunlin, Taiwan in 1997. He received the B.S. in department of mechanical engineering from National Taiwan University in 2019 and the M.S. degree in department of electrical engineering from National Taiwan University in 2021. He worked as a robot manipulator R.D. intern in Industrial Technology Research Institute (ITRI), Hsinchu, Taiwan when studying the M.S. degree from 2020 to 2021. His research majors in motion control of manipulators as well as machine vision.

Feng-Li Lian received the B.S. and M.S. degrees from National Taiwan University in 1992 and 1994, respectively, and the Ph.D. degree from the University of Michigan in 2001.Since 2002 he has been in the Department of Electrical Engineering, NTU, and since 2015 he also holds a joint appointment with Industrial Technology Research Institute, Hsinchu, Taiwan. From 2001 to 2002, he was a postdoctoral scholar at California Institute of Technology, and from 2009 to 2013, he was also the Division Director of Information Management, Computer & Information Networking Center, NTU. He is the recipient of the Youth Automatic Control Engineering Award from Chinese Automatic Control Society,

Taiwan, in 2007, the Outstanding Youth Award from Taiwan Association of System Science and Engineering in 2012, the Dr. Wu, Da-You Memorial Research Award, National Science Council, Taiwan, in 2012, the Excellent Young Scholar Research Grant, National Science Council, Taiwan, in 2012-14, and the NTU Excellent Teaching Award in 2007, 2008, 2010-2013, 2018, and 2019. His current research interests include distributed and networked control systems, multiple dynamical agent systems, trajectory generation and path planning for autonomous vehicles.

Yuan-Chieh Lo was born in 1992. He received his B.S. degree from Department of Mechanical Engineering, National Chiao-Tung University, the M.S. from Institute of Applied Mechanics, National Taiwan University in 2015 and 2017 respectively. He is currently an associate research fellow in Industrial Technology Research Institute. His main research interests are robotic simulation software, sensor-based control of industrial robots and autonomous system.

Chih-Hsuan Shih was born in 1989. He received his B.S. from National Taipei University of Technology, Taipei, Taiwan, R.O.C., in 2011, and his M.S. in bio-Industrial mechatronics engineering from the National Taiwan University Taipei, Taiwan, 2013. Since 2013 and 2021, he has been with the Mechanical and Mechatronics Systems Research Laboratories, Industrial Technology Research Institute (ITRI), where he was researcher and manager. His research interests are motion control of manipulators, simulation of manipulators, machine learning and deep learning, as well as machine vision.

Ming-Hau Tsai was born in 1980. He received his Ph.D. degree from Department of Mechanical Engineering, National Central University in 2011. He is currently a senior engineer in Industrial Technology Research Institute. His main research interests are robotics, motion control, and autonomous system.

Ping-Lang Yen was born in 1966. He received his B.S. degree from Department of Power Mechanical Engineering, National Tsing-Hua University, the M.S. degree from Department of Mechanical Engineering, National Taiwan University, and the PhD. degree from Department of Mechanical Engineering, Imperial College, London in 1998, 1990 and 1996 respectively. He is currently an assistant professor in the Department of Bio-Industrial Mechatronics Engineering, National Taiwan University. His main research interests are mechatronic control systems, medical robotics, and computer-assisted orthopaedic surgery.